1 # Transcriptomic atlas of mushroom development highlights an
2 # independent origin of complex multicellularity

3 Krisztina Krizsán[1], Éva Almási[1], Zsolt Merényi[1], Neha Sahu[1], Máté Virágh[1], Tamás Kószó[1],
4 Stephen Mondo[2], Brigitta Kiss[1], Balázs Bálint[1,3], Ursula Kües[4], Kerrie Barry[2], Judit Cseklye[3]
5 Botond Hegedűs[1,5], Bernard Henrissat[6], Jenifer Johnson[2], Anna Lipzen[2], Robin A. Ohm[7], István
6 Nagy[3], Jasmyn Pangilinan[2], Juying Yan[2], Yi Xiong[2], Igor V. Grigoriev[2], David S. Hibbett[8], László
7 G. Nagy[1*]

10 *1 Synthetic and Systems Biology Unit, Institute of Biochemistry, BRC-HAS, Szeged, 6726,*
11 *Hungary.*
12 *2 US Department of Energy (DOE) Joint Genome Institute, Walnut Creek, CA, 94598, United*
13 *States.*
14 *3 Seqomics Ltd. Mórahalom, Mórahalom 6782, Hungary*
15 *4 Division of Molecular Wood Biotechnology and Technical Mycology, Büsgen-Institute,*
16 *University of Göttingen, Göttingen, Germany.*
17 *5 Institute of Biophysics, BRC-HAS, Szeged, 6726, Hungary.*
18 *6 Architecture et Fonction des Macromolécules Biologiques (AFMB), UMR 7257 CNRS*
19 *Université Aix-Marseille, 13288, Marseille, France.*
20 *7 Department of Biology, Microbiology, Utrecht University, 3584 Utrecht, The Netherlands*
21 *8 Biology Department, Clark University, 01610 Worcester MA, USA*

24 *To whom correspondence should be addressed: lnagy@fungenomelab.com

27 **We constructed a reference atlas of mushroom formation based on developmental**
28 **transcriptome data of six species and comparisons of >200 whole genomes, to elucidate**
29 **the core genetic program of complex multicellularity and fruiting body development in**
30 **mushroom-forming fungi (Agaricomycetes). Nearly 300 conserved gene families and >70**
31 **functional groups contained developmentally regulated genes from five to six species,**
32 **covering functions related to fungal cell wall (FCW) remodeling, targeted protein**
33 **degradation, signal transduction, adhesion and small secreted proteins (including**
34 **effector-like orphan genes). Several of these families, including F-box proteins, protein**
35 **kinases and cadherin-like proteins, showed massive expansions in Agaricomycetes, with**
36 **many convergently expanded in multicellular plants and/or animals too, reflecting broad**
37 **genetic convergence among independently evolved complex multicellular lineages. This**
38 **study provides a novel entry point to studying mushroom development and complex**
39 **multicellularity in one of the largest clades of complex eukaryotic organisms.**

42   Mushroom-forming fungi (Agaricomycetes, Basidiomycota) represent an independent lineage of
43   complex multicellular organisms with a unique evolutionary history compared to complex
44   animals, plants and stramenopiles. They comprise >21,000 species and originated ~350 million
45   years ago[1], approximately coinciding with the origin of tetrapods. Mushrooms have immense
46   importance in agriculture, ecology and medicine; they represent an important and sustainable
47   food source, with favorable medicinal properties (e.g. antitumor, immunomodulatory)[2].
48   Complex multicellular development in fungi has been subject to surprisingly few
49   studies[3–6], resulting in a paucity of information on the genetic underpinnings of the independent
50   origins of complex multicellularity in fungi[7]. As complex multicellular structures, fruiting bodies
51   deploy mechanisms for hypha-to-hypha adhesion, communication, cell differentiation, defense
52   and execute a developmental program that results in a genetically determined shape and
53   size[6,7]. Fruiting bodies shelter and protect reproductive cells and facilitate spore dispersal.
54   Uniquely, complex multicellularity in fungi comprises short-lived reproductive organs whereas in
55   animals and plants it comprises the reproducing individual. Nevertheless, fruiting bodies evolved
56   complexity levels comparable to that of simple animals, with up to 30 morphologically
57   distinguishable cell types described so far. Fruiting body development is triggered by changing
58   environmental variables (e.g. nutrient availability), and involves a transition from simple
59   multicellular hyphae to a complex multicellular fruiting body initial. The initial follows genetically
60   encoded programs to develop species-specific morphologies[5,6], which in the Agaricomycetes
61   ranges from simple crust-like forms (e.g. *Phanerochaete*) to the most complex toadstools (e.g.
62   *Agaricus bisporus*). Previous studies identified several developmental genes, including
63   hydrophobins[8], defense-related proteins[9], fungal cell wall (FCW) modifying enzymes[10–13],
64   transcriptional regulators[4,5,14] (e.g. mating genes) and light receptors[15] (e.g white collar
65   complex). It is not known, however, what genes comprise the 'core toolkit' of multicellularity and
66   development in the Agaricomycetes.
67   Here we investigate the general evolutionary and functional properties of fruiting body
68   development and assess whether mushroom-forming fungi evolved complex multicellularity via
69   unique or convergent solutions, compared to other complex lineages (e.g. plants, animals or
70   brown algae). We combine comparative analyses of developmental transcriptomes of six
71   species with comparisons of 201 whole genomes and focus on conserved developmental
72   functions and complex multicellularity.
73
74
75   **Results**
76   We obtained fruiting bodies in the laboratory or from the field and profiled gene expression in 3-
77   9 developmental stages and tissue types for *Coprinopsis cinerea* AmutBmut*, Schizophyllum*
78   *commune* H4-8*, Phanerochaete chrysosporium* RP78*, Rickenella mellea* SZMC22713 and
79   *Lentinus tigrinus* RLG9953-sp. We used data for *Armillaria ostoyae* C18/9 from our previous
80   work[16]. We report the *de novo* draft genome of *Rickenella mellea* (Hymenochaetales), the
81   phylogenetically most distant species from *Coprinopsis* in our dataset, spanning >200 million
82   years of evolution[1]. To construct a reference atlas of mushroom development, we performed
83   poly(A)+ RNA-Seq on Illumina platforms, in triplicates (totalling to >120 libraries, Supplementary
84   Table 1). We obtained an average of 60.8 million reads per sample, of which on average 83.3%
85   mapped to the genomes (Supplementary Fig 1). For each species, the first and last

86   developmental stage sampled were vegetative mycelium and mature fruiting body at the time of
87   spore release, respectively. This spans all developmental events of fruiting bodies except
88   senescence. Because it is difficult to align intermediate developmental stages across species,
89   we identified developmentally regulated genes using an approach that removes developmental
90   stage identity from the analyses (see Methods). Using this strategy, we could recover >80% of
91   previously reported developmental genes of *Coprinopsis* (Supplementary Table 2). To more
92   broadly infer functionalities enriched in mushroom forming fungi, we analyzed Interpro domain
93   counts across 201 fungal genomes (including 104 Agaricomycetes), which revealed 631
94   significantly overrepresented domains in mushroom-forming fungi ($P < 0.01$, Fisher exact test,
95   abbreviated FET, Supplementary Table 3-4).
96

Dynamic reprogramming of the fungal transcriptome

98   We detected 12,003 - 17,822 expressed genes, of which 938-7,605 were developmentally
99   regulated in the six species (Fig. 1/a, Supplementary Table 5). We found 192-7,584 genes that
100   showed significant expression dynamics during fruiting body development ('FB' genes). Of
101   developmentally regulated genes 188-1,856 genes were upregulated at fruiting body initiation
102   ('FB-init' genes), which represents a transition from simple to complex multicellular organization.
103   Only *Phanerochaete chrysosporium* had more FB-init genes than FB genes, which is consistent
104   with its fruiting bodies being among the least complex types in the Agaricomycetes. The number
105   of genes significantly differentially expressed (DEG) at fruiting body initiation further suggests
106   that the transition to complex multicellularity is associated with a major reprogramming of gene
107   expression (Supplementary Fig. 2). The largest numbers of DEGs were observed in cap and gill
108   tissues in all four species with complex fruiting bodies. On the other hand, the expression
109   profiles of stipes changed little relative to primordium stages of *Armillaria, Lentinus* and
110   *Rickenella*, which is explained by the differentiation of the cap initial at the top of a primordial
111   stipe, as opposed to *Coprinopsis*, in which stipe and cap differentiation happens simultaneously
112   inside the fruiting body initial[17]. Many Gene Ontology (GO) terms were partitioned between
113   vegetative mycelium and fruiting body samples (P<0.05, FET). Terms related to fungal cell wall,
114   oxidoreductase activity and carbohydrate metabolism were enriched in developmentally
115   regulated genes of all six species (Fig. 1/b, Supplementary Table 6), suggesting that cell wall
116   remodeling is a common upregulated function in fruiting bodies. Other commonly enriched
117   terms cover functions such as DNA replication, transmembrane sugar transport, ribosome,
118   membrane and lipid biosynthesis, while many other were specific to single species
119   (Supplementary Fig. 3).
120   To obtain a higher resolution of developmental events, we arranged developmentally
121   regulated genes into co-expression modules using the Short Time Series Expression Miner
122   (STEM)[18]. Developmentally regulated genes grouped into 28-40 modules, except
123   *Phanerochaete* which had eleven. The largest modules in all species contained genes
124   expressed at fruiting body initiation or in early primordia and genes with tissue-specific
125   expression peaks, in young fruiting body caps, gills, stipes, mature fruiting bodies and stipes or
126   caps (Fig 1/c; for further data see Supplementary Fig. 4 and Supplementary Note 1). Many
127   early-expressed modules show upregulation across multiple stages (hyphal knot, stage 1 and 2
128   primordia), suggestive of an early expression program overarching multiple primordium stages.

Co-expression modules display distinct functional enrichment signatures, as shown on Fig 1/c and Supplementary Table 7. For example, DNA replication and mitosis were characteristic for early-expressed modules, consistent with an early wave of nuclear and cellular division events followed by cell expansion without significant change in cell numbers[5]. Growth by cell expansion is a mechanism shared with plants and possibly reflects constraints imposed by independently evolved rigid cell walls in these groups.
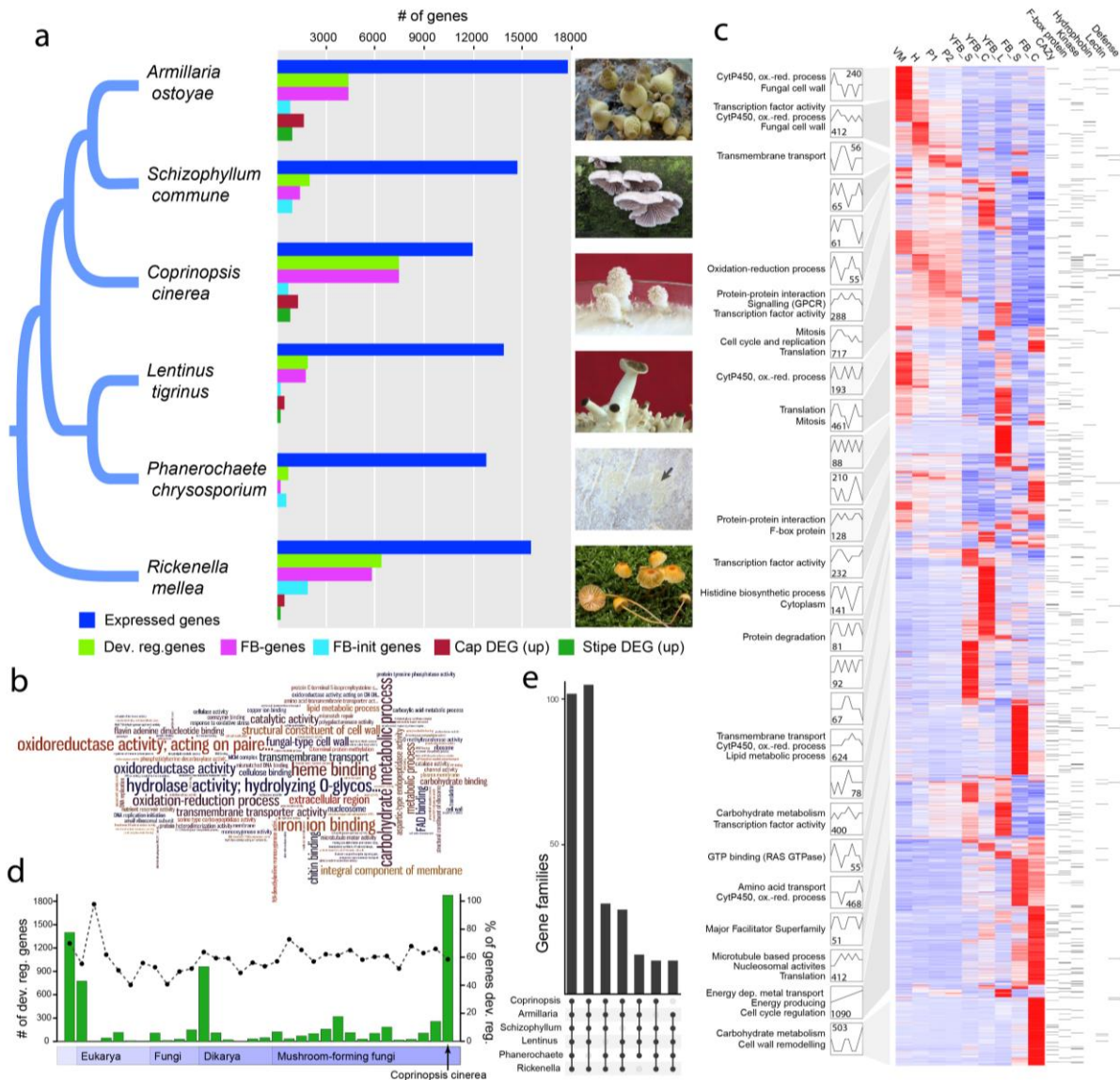
Fig. 1. Overview of the developmental transcriptomes, **a**, the distribution of developmentally regulated and cap and stipe differentially expressed (DEG) genes in six mushroom-forming species. Fruiting bodies are shown on the right (*Phanerochaete*: K. Krizsán, *Rickenella:* Bálint Dima, others: L.G. Nagy). Two groups of developmentally regulated genes were defined: those that show >4 fold change and a FPKM>4 between any two stages of fruiting body development (referred to as 'FB genes') and that show >4 fold increase in expression from vegetative mycelium to the first primordium stage (referred to as 'FB-init genes'). These definitions exclude

144   genes that show highest expression in vegetative mycelium and little or no dynamics later on. **b**,

145   wordcloud of Gene Ontology terms enriched in the developmentally regulated genes in the six

146   species. Word size corresponds to the number of species in which a term was significantly

147   enriched (*P* < 0.05, Fisher exact test). **c**, Analysis of co-expression modules in *Coprinopsis*

148   *cinerea*. Heatmap of 7475 developmentally expressed genes arranged based on module

149   assignment, with simplified expression profiles and the GO enrichment terms given for each

150   module (see also Supplementary Table 7). We graphically depict only 27 modules with >50

151   genes (refer to Supplementary Fig. 4 for the complete list and data for other species). The

152   distribution of key developmental genes is given on the right side of the heatmap. **d**,

153   Phylostratigraphic profile of developmentally regulated genes of *Coprinopsis cinerea*. Genes are

154   divided into age categories from genes shared by all cellular life (left) to species-specific genes

155   (right). The percentage of developmentally regulated genes compared to all genes in a category

156   is shown by a dashed line. Data for other species is presented in Supplementary Fig. 5. **e**,

157   UpSetR representation of gene families developmentally regulated in at least 5 species. See
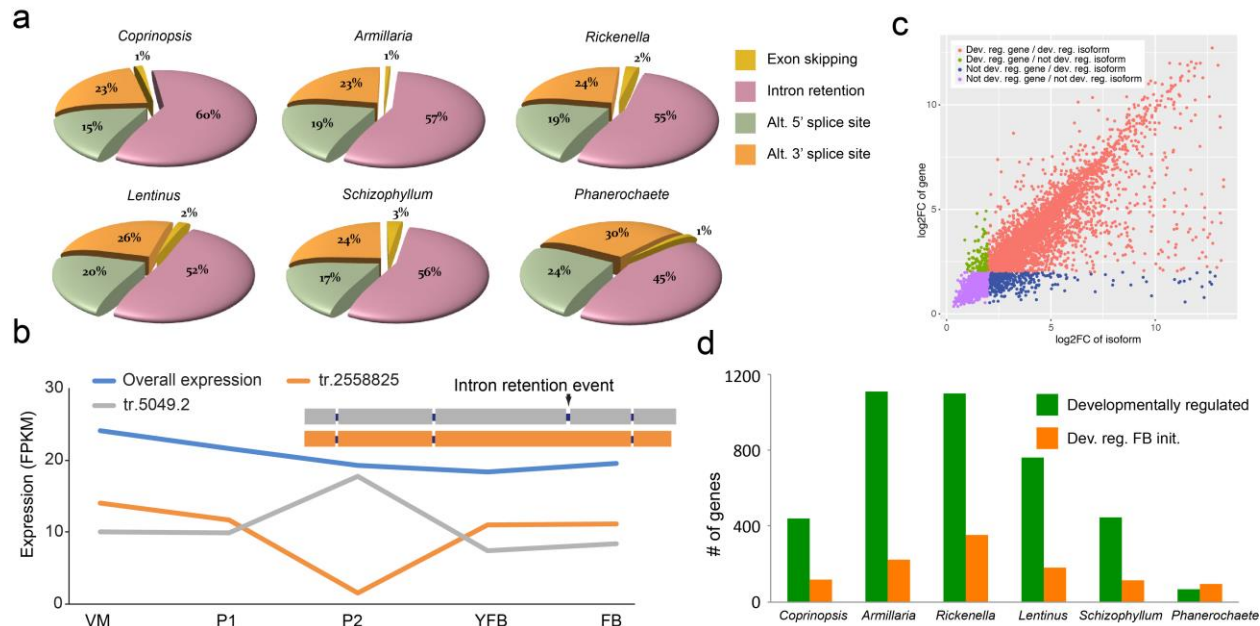
158   also Supplementary Fig. 6.

Most developmental gene families are older than fruiting body formation

160   We investigated the evolutionary age distribution of developmentally regulated genes using

161   phylostratigraphy[19], based on a dataset of 4,483 archaeal, bacterial and eukaryotic genomes[20]

162   supplemented with 416 fungi (of which 113 were Agaricomycetes). We assigned genes to

163   phylogenetic ages, 'phylostrata', by identifying for each gene the most phylogenetically distant

164   species in which a homolog could be detected. The phylostratigraphic profiles of all species

165   show three peaks, corresponding to two major periods of fungal gene origin: the first containing

166   genes shared by all living species, the second by the Dikarya (Ascomycota + Basidiomycota)

167   and a third containing species-specific genes. Many developmentally regulated genes have

168   homologs in simple multicellular and unicellular eukaryotes and prokaryotes: the origin of 49.3 -

169   63.3% predate the origin of mushroom-forming fungi (Fig. 1/d, Supplementary Fig. 5), indicating

170   that co-option of conserved genes contributed significantly to the evolution of fruiting bodies.

171   Nevertheless, Agaricomycetes-specific phylostrata showed a characteristic enrichment for F-

172   box genes, transcription factors and protein kinases, indicating an increased rate of origin for

173   these in mushroom-forming fungi (Supplementary Table 8).

Splicing patterns associate with development

175   We reconstructed transcript isoforms across developmental stages and tissue types in the six

176   species using region restricted probabilistic modeling, a strategy developed for gene-dense

177   fungal genomes[21]. We found evidence of alternative splicing for 36-46% of the expressed genes

178   (Supplementary Table 9), which is significantly higher than what was reported for fungi outside

179   the Agaricomycetes[22,23] (1-8%). This transcript diversity was generated by 6,414 - 13,780

180   splicing events in the six species. Of the four main types of events, intron retention (44.3-60.5%)

181   was the most abundant in all species, followed by alternative 3' splice site (22.9-30.1%),

182   alternative 5' SS (15.6-24.1%) and exon skipping (0.8-2.9%) (Fig. 2/a), consistent with

183   observations made on other fungi[22–24]. No substantial difference in the proportion of spliced

184   genes and of splicing events was observed across developmental stages, tissue types or

185 species. Nevertheless, we found that several genes with nearly constant overall expression
186 level had developmentally regulated transcript isoforms (Fig 2/b-c). The six species had 159-
187 1,278 such genes, the highest number in *Rickenella* (1,278) and the lowest in *Phanerochaete*
188 (159) (Fig 2/d, Supplementary Table 9). Based on their expression dynamics, these transcripts
189 potentially also contribute to development, expanding the space of developmentally regulated
190 genes through alternative splicing.
191

193 **Fig. 2.** Splicing patterns through fruiting body development. **a**. distribution of four main
194 alternative splicing events across species (see also Supplementary Table 9). **b**. Genes with little
195 dynamics can contain developmentally regulated transcripts, Schco3_2558825 is shown here
196 as an example **c**. Scatterplot of gene versus transcript expression dynamics in *Coprinopsis*
197 *cinerea*, highlighting developmentally regulated transcripts (red). Plotted are fold change values
198 between the minimum and maximum expression across all developmental stages for genes (y
199 axis) and alternative transcript (x axis). Developmentally regulated transcripts (i.e. those that
200 show FC>4 across any two developmental stages and FPKM>4) of non-developmentally
201 regulated genes (FC<4) are highlighted in red. **d**. bar plot of developmentally regulated
202 transcripts that were detected within not developmentally regulated genes.

Conserved transcriptomic signatures of mushroom development

204 Our transcriptome data are particularly suited to detecting shared patterns of gene expression
205 across species. We analyzed common functional signals in the six species by estimating the
206 percent of developmentally regulated genes shared by all or subsets of the species based on
207 Markov clustering[25] of protein sequences. We found 100 clusters containing developmentally
208 regulated genes from all six species, and 196 in five species (Fig. 1/e, Supplementary Table
209 10). These are enriched for GO terms related to oxidation-reduction processes, oxidoreductase
210 activity, carbohydrate metabolism, among others, corresponding to a suite of carbohydrate
211 active enzymes. Of the 100 families shared by 6 species, fifteen can be linked to the fungal cell

6

212   wall (FCW), while the remaining families cover diverse cellular functions such as
213   transmembrane transport (6 families), cytochrome p450s (5 families), targeted protein
214   degradation (5 families), or peptidases (3 families). One hundred and four gene families are
215   shared by five species excluding *Phanerochaete* (Fig 1/e), which comes as no surprise, as this
216   species produces the simple crust-like, fruiting bodies. Besides these highly conserved families,
217   an additional 73 functional groups of genes are developmentally regulated in six or five species,
218   but didn't group into gene families due to their higher rate of evolution. These include most
219   transcription factors, kinases, aquaporins, certain peptidase families and enzymes of primary
220   carbohydrate metabolism (trehalose and mannitol, Supplementary Figure 8) among others
221   (Supplementary Table 10).
222   Shared developmentally regulated gene families included a conserved suite of CAZymes
223   active on the main chitin and β-1,3- and β-1,6- glucan polymers as well as minor components of
224   the FCW. These included various glycoside hydrolases (GH), hydrophobins, expansin-like
225   proteins and cerato-platanins, among others. A large suite of β-glucanases, chitinases,
226   laccases, endo-β-1,4-mannanases, α-1,3-mannosidases were developmentally regulated, many
227   of which are also expanded in Agaricomycetes (Table 1, Supplementary Fig 7). The expression
228   of glucan-, chitin- and mannose-active enzymes is consistent with active FCW remodeling
229   during fruiting body formation and recent reports of similar genes upregulated in the fruiting
230   bodies of *Lentinula*[12,13,26], *Flammulina*[27] and *Coprinopsis*[28]. Kre9/Knh1 homologs are
231   developmentally regulated in all species and are overrepresented in mushroom-forming fungi (P
232    $= 1.45 \times 10^{-5}$, FET). This family is involved in β-glucan assembly in *Saccharomyces* and has
233   putative signaling roles through an interaction with MAP kinases[29]. Although generally linked to
234   cellulose degradation[30,31], expansins, lytic polysaccharide monooxygenases and cellobiose
235   dehydrogenases have recently been shown to target chitin polymers[32,33] or are expressed in
236   fruiting bodies of *Pycnoporus*[34] and *Flammulina*[35], suggesting a role in fruiting body
237   development. In addition, developmental expression of two alginate lyase-like families (Table 1)
238   were shared by 6 species and that of a β-glucuronidase (GH79_1) was shared by 4 species
239   (*Armillaria, Coprinopsis, Rickenella* and *Lentinus*). While the targets of these families in fruiting
240   bodies are currently unknown, their conserved expression pattern suggests roles in
241   polysaccharide metabolism during development[36]. Comparison across 201 genomes revealed
242   that 24 of these families have undergone expansions in the Agaricomycetes (Table 1,
243   Supplementary Table 3). In summary, CAZymes might be responsible for producing fruiting
244   body-specific FCW architectures, confer adhesive properties to neighboring hyphae or plasticity
245   for growth by cell expansion. We, therefore, suggest that FCW remodeling comprises one of the
246   foundations of the transition to complex multicellularity during the life cycle of fungi.
247   A significant fraction of conserved developmentally regulated genes carry extracellular
248   secretion signals and were predicted to be glycosylphosphatidylinositol (GPI) anchored (Fig 3/a,
249   Supplementary Fig. 9). These include diverse FCW-active proteins, such as laccases (AA1),
250   glucanases (GH5, GH16, Kre9/Knh1 family), chitooligosaccharide deacetylases, but also
251   lectins, A1 aspartic peptidases and sedolisins, among others (Supplementary Table 11). GPI-
252   anchored proteins often mediate adhesion in filamentous and pathogenic fungi[37], but it is not
253   known whether similar mechanisms are at play in fruiting bodies[7]. Laccases and glucanases
254   could facilitate adhesion by oxidative crosslinking or other covalent modifications of neighboring
255   hyphal surfaces, although more data is needed on the biochemistry involved. Nevertheless, it

7

256   seems safe to conclude that FCW-active proteins may bind neighboring hyphae through
257   covalent FCW modifications in fruiting bodies, which would represent a unique adhesion
258   mechanism among complex multicellular organisms. Homologs of cadherins (adhesive proteins
259   of animals) are enriched in Agaricomycetes compared to other fungi (P = 1.1x10^{-4}, FET) and
260   were developmentally regulated in all species. Although fewer in numbers than in animals, their
261   convergent expansion in complex multicellular fungi and metazoans could indicate recurrent co-
262   option for developmental functions.

263   Fruiting body secretomes contained a rich suite of genes encoding small secreted
264   proteins (SSPs, <300 amino acids, with extracellular secretion signal). Of the 190-477 SSPs
265   predicted in the genomes of the six species, 20-61% are developmentally regulated, with ~20%
266   being conserved across the six species (Fig. 3/b Supplementary Fig. 10). Conserved and
267   annotated genes comprise various FCW-related families, such as hydrophobins, cerato-
268   platanins, cupredoxins, lectins, Kre9/Knh1, GH12 and LysM domain proteins, among others
269   (Fig. 3/c, Supplementary Fig. 11). Hydrophobins and cerato-platanins are SSPs that self-
270   assemble into a rodlet layer on the cell surface, confer hydrophobic surfaces to hyphae that
271   hinder soaking of fruiting bodies with water. They are hypothesized to mediate adhesion, the
272   aeration of fruiting bodies[8,38], or pathogenicity[39]. As reported previously[8], most hydrophobin
273   genes are developmentally regulated (Fig. 3/d) and the family is overrepresented in the
274   genomes of mushroom-forming fungi (P < 10^{-300}, FET). Cerato-platanins are also expanded (P =
275   1.56x10^{-50}, FET) and developmentally regulated (except in *Phanerochaete*). In addition to
276   conserved genes, >40% of developmentally regulated SSPs had no functional annotations
277   and/or were species-specific orphans (Fig. 3/c). This proportion is similar to that observed in
278   ectomycorrhiza-induced SSPs[1,40] and suggests that species-specific secreted proteins have a
279   role also in fruiting body development. Although their function in fruiting bodies is not known,
280   their role in signaling across partners in ectomycorrhizal[40] and pathogenic interactions[41], or
281   within species[42,43], raises the possibility that some of the detected SSPs might act as fruiting
282   body effectors. This could also explain the rich SSP repertoires of saprotrophic
283   Agaricomycetes[44].
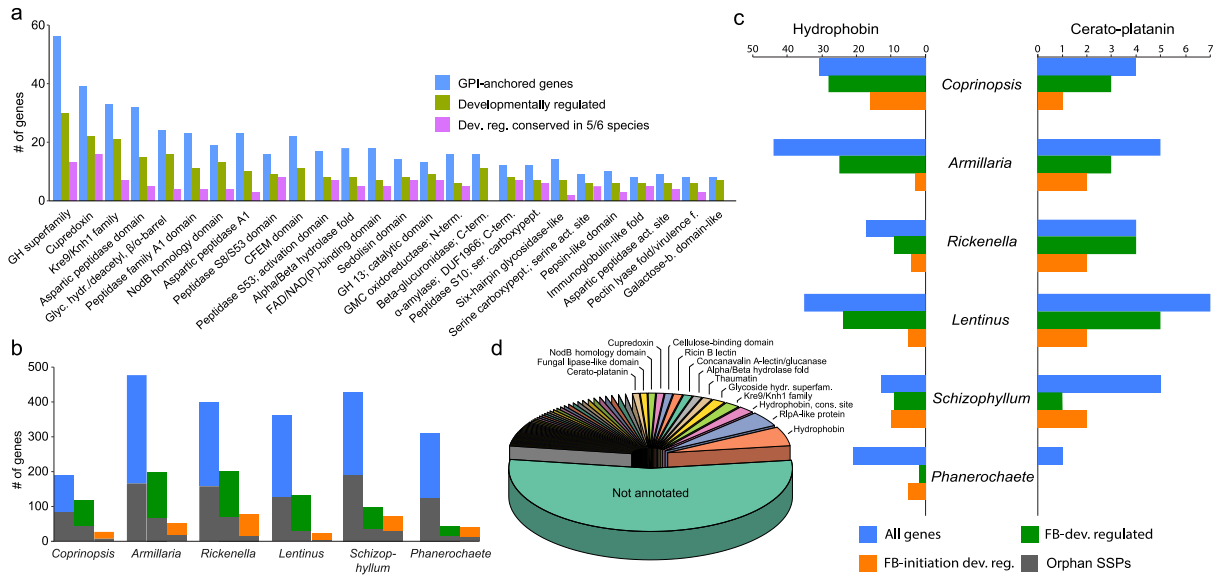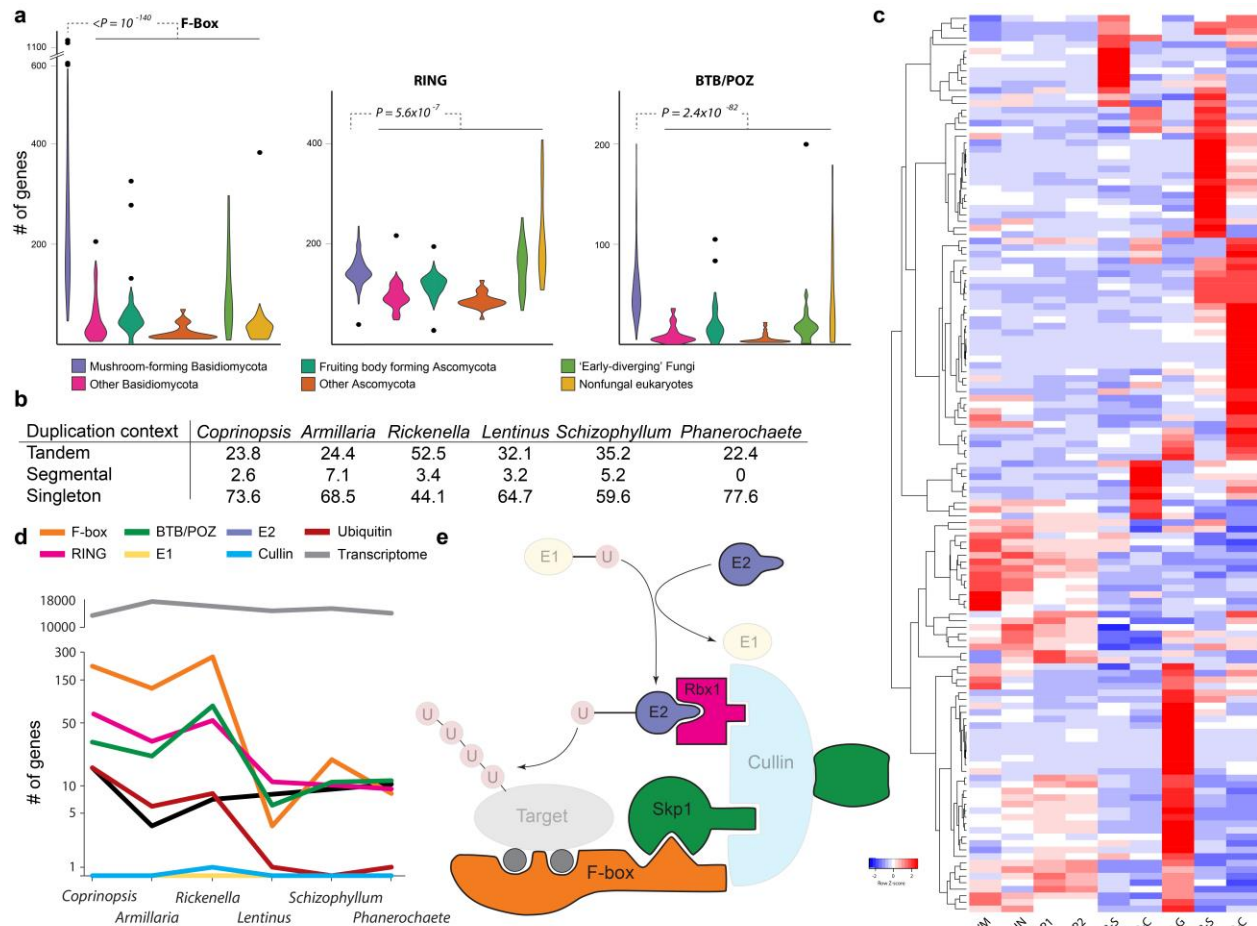
Fig. 3. Diverse secreted proteins are developmentally regulated in fruiting bodies. **a**. the distribution of GPI-anchored secreted protein repertoire, its developmentally regulated and conserved developmentally regulated subsets. **b**. Numbers of all and developmentally regulated small secreted proteins, with orphan genes shaded differently. **c**. Copy number distribution and developmental regulation of hydrophobins and cerato-platanins in the six species. **d**. Functional annotation of small secreted proteins in the six species.

Targeted protein degradation shows striking expansion in mushrooms

We found a strong signal for developmental expression of components the E3 ubiquitin ligase complex. Several genes encoding F-box proteins, RING-type zinc-finger and BTB/POZ domain proteins are developmentally regulated in all species, often displaying tissue or developmental stage-specific expression peaks (Fig. 4, Supplementary Fig. 12). These gene families are also strongly overrepresented in the genomes of mushroom-forming fungi compared to related filamentous fungi and yeasts (Fig 4/a). For example, while yeasts and filamentous fungi possess ~20 and 60-90 F-box proteins[45], respectively, mushroom-forming fungi have 67-1,199 copies (mean: 274), comparable to the numbers seen in higher plants[46] and resulting predominantly from recent tandem duplications (Fig. 4/b, Supplementary Fig. 13). They mostly showed a single peak in expression and many of them were upregulated at fruiting body initiation or in caps, gills and stipes (Fig 4/c).The numbers of developmentally regulated F-box, RING-type zinc-finger and BTB/POZ domain containing genes found in the six species show a good correlation with fruiting body complexity but a poor correlation with the number of expressed genes (Fig 4/d), suggesting a link between the expansion of these genes and the evolution of complex fruiting body morphologies. These genes define the target specificity of E3 ubiquitin ligases[45,47], which enables a tight regulation of selective proteolysis during development[46]. In plants, F-box proteins can also act as transcriptional regulators[48], although this is yet to be proven in fungi. On the other hand, ubiquitin conjugating (E2) enzymes are developmentally regulated only in *Coprinopsis, Armillaria* and *Rickenella*, whereas ubiquitin activating (E1) enzymes, cullins,

9

312 SKP1, HECT-type ubiquitin ligases are neither developmentally regulated nor significantly
313 overrepresented in mushroom-forming fungi (Fig 4/e, P > 0.05, FET). With the exception of
314 *Coprinopsis*, we did not detect specific expression patterns of neddylation and deneddylation
315 genes as reported for the Ascomycota[49]. Taken together, we observed a striking expansion and
316 distinctive expression patterns of genes that define target-specificity of the E3 ubiquitin ligase
317 complex (F-box, RING and BTB/POZ proteins) in Agaricomycetes. This parallels F-box gene
318 expansion in plants which, combined with their widespread role in development[46,50], suggests
319 that they likely have key roles in complex multicellular development in mushroom-forming fungi.
320

Duplication context	Coprinopsis	Armillaria	Rickenella	Lentinus	Schizophyllum	Phanerochaete
Tandem	23.8	24.4	52.5	32.1	35.2	22.4
Segmental	2.6	7.1	3.4	3.2	5.2	0
Singleton	73.6	68.5	44.1	64.7	59.6	77.6

321
322 Fig. 4. **a**, Copy number distribution of F-box, RING-type zinc finger and BTB/POZ domain
323 proteins showing their enrichment in mushroom-forming fungi compared to other fungal groups.
324 **b**, The context of gene duplications of F-box proteins in the genomes of six analyzed species. **c**,
325 heatmap of developmentally regulated F-box proteins in *Coprinopsis cinerea*. Genes were
326 hierarchically clustered based on gene expression similarity using average linkage clustering.
327 Abbreviations: VM - vegetative mycelium, HN - hyphal knot, P1 - stage 1 primordium, P2 - stage
328 2 primordium, YFB - young fruiting body, FB - mature fruiting body, '-C' - cap, '-S' - stipe, '-G' -
329 gills. **d**, The correlation between morphological complexity of fruiting bodies and the number of
330 developmentally regulated elements of the E3 ligase complex. **e**, Outline of the E3 ubiquitin
331 ligase complex highlighting members expanded and developmentally regulated (solid) in

10

332 mushroom-forming fungi. Transparent members are not expanded nor developmentally
333 regulated.

Key multicellularity-related genes are developmentally regulated in fruiting bodies

336 Complex multicellularity in fungi is implemented by the reprogramming of hyphal branching
337 patterns, followed by their adhesion and differentiation[7]. This assumes mechanisms for cell-to-
338 cell communication, adhesion, differentiation and defense. We examined the expression
339 dynamics of gene families related to these traits, including transcription factors (TFs), protein
340 kinases, adhesion and defense-related genes. Like other complex multicellular lineages,
341 mushroom-forming fungi make extensive use of transcription factors (TFs) in development. To
342 identify development-related TFs, we manually curated TF candidate genes to exclude ones
343 that nonspecifically bind DNA. The resulting TFomes contain 278-408 genes, of which 4.5-64%
344 were developmentally regulated (Supplementary Fig. 14). These were dominated by C2H2 and
345 Zn(2)C6 fungal type, fungal trans and homeodomain-like TFs (Fig 5/a). Although transcription
346 factor families were usually not conserved, we found 5 TF families that contained
347 developmentally regulated genes from 5 or 6 species (Supplementary Table 10). These
348 included C2H2-type zinc fingers (including *c2h2* of *Schizophyllum*[14,51]), Zn(2)-C6 fungal-type
349 and homeobox TFs (containing *hom1* of *Schizophyllum*[14,51]). Two clusters of C2H2 and
350 homeobox TFs showed expression peaks in stipes of *Coprinopsis, Lentinus, Armillaria* and
351 *Rickenella*, confirming previous reports of *Hom1* expression in *Coprinopsis*[52] and
352 *Schizophyllum*[51,53]. Members of the white collar complex were developmentally regulated in all
353 species except *Phanerochaete*, mostly showing a significant increase in expression at initiation.
354 However, these genes did not group into one family in the clustering, which was a common
355 pattern for TF families, perhaps caused by their high rate of sequence evolution.
356   Communication among cells by various signaling pathways is paramount to the increase
357 of distinct cell types in evolution. In accordance with the higher complexity of mushroom-forming
358 fungi, their kinomes are significantly larger than that of other fungi (P = 1.1×10^{-184}, FET, Fig 5/b),
359 due to expansions of the eukaryotic protein kinase superfamily. We classified protein kinases
360 into nine groups[54] using published kinome classifications for *Coprinopsis*[3]. The six mushroom
361 kinomes (Supplementary Table 12) have a similar composition, with PKL, CMGC and CAMK
362 families being most diverse and RGC and tyrosine kinases missing. The Agaricomycetes-
363 specific FunK1 family is expanded significantly, as reported earlier[3]. Tyrosine kinase-like
364 kinases also show a strong expansion in Agaricomycetes (P < 10^{-300}), consistent with
365 observations in *Laccaria bicolor*[55] and other species[56]. Histidine kinases are underrepresented
366 (P = 8.95×10^{-36}) relative to other fungal groups.
367   A kinase co-expression network revealed tissue specificity as the main driver of network
368 topology (Fig 5/c-d), with most kinases showing an expression peak late in development.
369 Kinases with early expression peaks are mostly highly expressed through multiple stages,
370 resembling early expressed modules of *Coprinopsis* (Fig. 1/c, Supplementary Fig. 15). Many
371 CAMK family members showed expression peaks in cap and gill tissues. However, overlaying
372 the network with classification shows no general enrichment of any family in developmental
373 stages or tissues (Fig 5/d-e), indicating diverse co-option events for development at the highest

11

374 level of kinase classification. The FunK1 family has been linked to multicellular development,
375 based on an upregulation in fruiting bodies[3]. In our species FunK1 comprises 4-33% of the
376 kinome and 0.2-35% of the developmentally regulated kinases, although this Fig. resembles
377 that of other kinase families. Members of the highly expanded tyrosine kinase like (TKL) family
378 (Fig 5/e) are developmentally regulated in *Coprinopsis*, *Armillaria* and *Rickenella*, but not in
379 species with simpler morphologies. The expansion and developmental expression of the TKL
380 family in mushroom-forming fungi is a remarkable case of convergence with complex
381 multicellular plants[57,58] and animals[58] and may be related to parallel increases in organismal
382 complexity. Yet, while most plant TKL genes have receptor-like architectures[59], we found no
383 evidence of extracellular domains or secretion signals in TKL genes of mushroom-forming fungi,
384 suggesting they orchestrate signal transduction via soluble kinases or other mechanisms
385 different from those of multicellular plants and animals.
386   Fungal immune systems comprise innate chemical defense mechanisms against
387 metazoan predators and bacterial and fungal infections[60]. We catalogued eleven families of
388 defense effector proteins and their expression to assess the conservation of the defensive
389 arsenal of Agaricomycetes. Genomes of mushroom-forming fungi harbor highly species-specific
390 combinations of defense-related genes encoding pore-forming toxins, cerato-platanins, lectins
391 and copsins, among others, with most of them being developmentally expressed and
392 upregulated at fruiting body initiation (Supplementary Fig 16). Of the eleven families only three
393 were conserved, and only one (thaumatins) was developmentally regulated in all six species,
394 which can display either endoglucanase or antimicrobial activity, depending on the structure of
395 the mature protein. *In silico* structure prediction identified an acidic cleft in fruiting body
396 expressed thaumatins (Supplementary Fig 16), consistent with an antimicrobial activity. Several
397 defense-related lectins have been reported from fruiting bodies[61], although lectins have been
398 implicated in cell adhesion and signaling too. Agaricomycete genomes encode at least 17 lectin
399 and 2 lectin-like families, of which seven are significantly overrepresented (P<0.05, FET,
400 Supplementary Table 3). Developmentally regulated lectins belong to nine families, with 4-7
401 family per species, but only ricin B lectins were developmentally regulated in all six species
402 (Supplementary Fig 17). Other lectin families show a patchy phylogenetic distribution, which is
403 also reflected in their expression patterns in fruiting bodies. Several lectins are induced at
404 fruiting body initiation, including all previously reported nematotoxic *Coprinopsis* lectins (CCL1-
405 2, CGL1-3 and CGL3). Taken together, the defense effector and lectin-encoding arsenal of
406 mushroom-forming fungi shows a patchy phylogenetic distribution, consistent with high gene
407 turnover rates or gains via horizontal gene transfer[60]. Accordingly, expressed defense gene sets
408 are highly species-specific, with most of the encoded genes upregulated in fruiting bodies,
409 suggesting that chemical defense is a key fruiting body function.
410
411

412
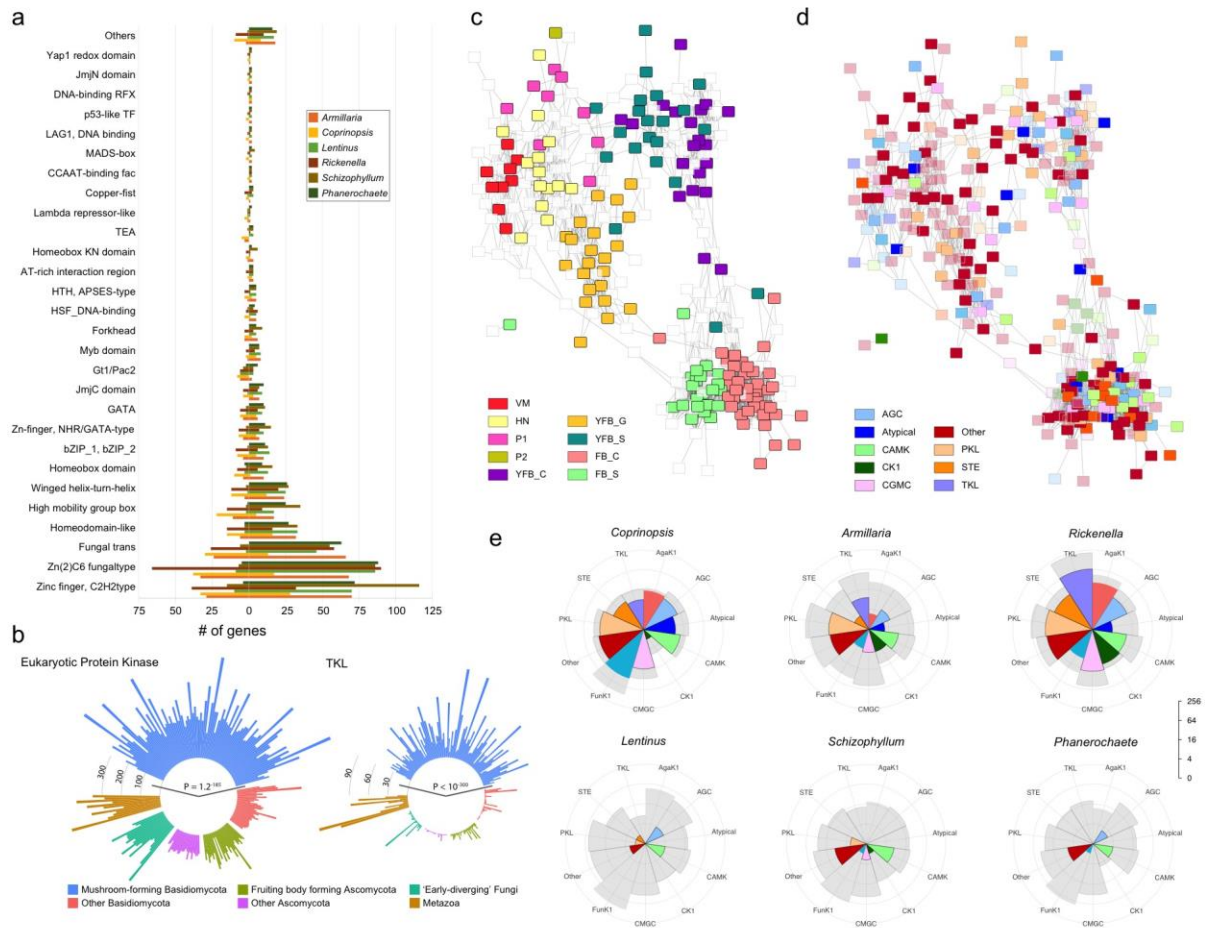
Fig. 5. Expression and copy number distribution of transcription factor and kinase genes. **a**. transcription factor family distribution and the proportions of developmentally regulated (left) versus not regulated (right) genes across six species. **b**. Circular bar diagram of eukaryotic protein kinase (left) and tyrosine kinase-like (right) repertoires of mushroom-forming fungi versus in other fungal groups and non-fungal eukaryotes. P values of overrepresentation in mushroom-forming fungi are given for both plots. **c** and **d**. Co-expression network of 306 expressed kinases of *Coprinopsis cinerea* overlaid with expression peak (**c**) and kinase classification (**d**). Pairwise correlation coefficients of expression profile similarity were calculated for each pair of kinase genes and networks were visualized with a correlation coefficient cutoff of 0.825. **e**. Kinome (grey fill) and developmentally regulated kinome (solid fill) repertoires of the six species split by kinase classification. The families Funk1 and Agak1 of the 'Other' group are shown separately. Axes are transformed to $\log_2$ scale.

Discussion

We charted the transcriptomic landscape of multicellular development in 6 phylogenetically diverse mushroom-forming species and performed comparative analyses of >200 genomes. We pinpointed nearly 300 conserved gene families, and another 73 gene groups with developmentally dynamic expression in ≥5 species, as well as 631 domains significantly overrepresented in mushroom-forming fungi. These are enriched in cell wall modifying

13

431 enzymes, various secreted proteins (including GPI-anchored and small secreted proteins),
432 components of the ubiquitin ligase complex, kinases or transcription factors. Lectins and
433 defense effectors, on the other hand, showed species-specific repertoires, indicating a higher
434 rate of evolutionary turnover. These data provide a framework for elucidating the core genetic
435 program of fruiting body formation and will serve as guideposts for a systems approach to
436 understanding the genetic bases of mushroom development and multicellularity.
437 Complex multicellularity evolved in five lineages, of which plants, animals and fungi are
438 the most diverse[7,58]. At the broadest level of comparison, these lineages evolved similar
439 solutions to cell adhesion, communication, long-range transport and differentiation[58,62,63]. As in
440 animals and plants, protein kinases, putative adhesive proteins, defense effectors, and certain
441 transcription factors have expanded repertoires in mushroom-forming fungi and show
442 developmentally dynamic expression patterns. Examples for convergent expansions in
443 mushroom-forming fungi, in plants and/or animals include TKL family kinases, F-box proteins
444 and cadherins, indicating that ancient eukaryotic gene families with apt biochemical properties
445 have been repeatedly co-opted for complex multicellularity during evolution. F-box proteins
446 showed the largest expansion in Agaricomycetes across all families and was the largest
447 developmentally regulated family, along with RING-type and BTB domain proteins. Among
448 independently evolved fruiting body forming fungi[7,49,64], Agaricomycetes share some similarity
449 with the Pezizomycotina (Ascomycota), many of which also produce marcoscopic fruiting
450 bodies. For example, laccases, lectins, several transcription factors and signal transduction
451 systems have also been implicated in fruiting body formation in the Pezizomycotina, although at
452 the moment it is unclear how frequently convergent expansions and co-option events can be
453 observed in independently evolved lineages of complex multicellular fungi[7].
454 Mushroom-forming fungi also show several unique solutions for multicellularity, as
455 expected based on their independent evolutionary origin. These are, in part, explained by the
456 very nature of fungi: complex multicellularity comprises the reproductive phase of the life cycle
457 (except in sclerotia, rhizomorphs) and so mechanisms have evolved for sensing when fruiting
458 body formation is optimal (e.g. nutrient availability, light). Mushroom development can be
459 partitioned into an early phase of cell proliferation and differentiation and a growth phase of
460 rapid cell expansion, a division evident on gene co-expression profiles as well. Broadly
461 speaking, this is similar to the development of fleshy plant fruits, although mechanisms are likely
462 to be convergent, like many other aspects of mushroom development.
463 This work has provided a glimpse into the core genetic toolkit of complex multicellularity
464 in mushroom-forming fungi. Our comparative transcriptomic genomic analyses revealed gene
465 families, most of which reported as novel, with conserved developmental expression in fruiting
466 bodies, with scope to increase the resolution both phylogenetically and among cell types (e.g.
467 by single-cell RNA-Seq). Such data should help defining the conserved genetic programs
468 underlying multicellularity in mushroom-forming fungi, and uncovering the evolutionary origins of
469 a major complex multicellular lineage in the eukaryotes.
470

471 ## Methods

472 **Strains, fruiting protocols and nucleic acid extraction**

473   For fruiting *Coprinopsis cinerea* strain #326 (*A43mut B43mut pab 1-1*) an agar disk (5 mm in
474   diameter) was placed on the center of YMG/T agar media (4 g yeast extract, 10 g malt extract, 4
475   g glucose, 10 g agar media with 100 mg tryptophane added after cooling[65]) at 37 °C for five
476   days in the dark. When the colonies reached the 1-2 mm distance from the edge of Petri dishes
477   they were placed into 25 °C for one week in a 12 hrs light/12 hrs dark cycle for fruiting. Fruiting
478   body stages were defined following standard conventions[5]. Exact alignment of developmental
479   stages across species was impossible, but we made an attempt to define functionally putatively
480   homogeneous stages to follow the general notation of mushroom developmental stages as
481   closely as possible in each species. Nevertheless, the array of sample types differed from
482   species to species, due to the morphological diversity of fruiting bodies or limitations in
483   dissectability. In *Coprinopsis*, vegetative mycelium, hyphal knot, stage 1 and stage 2 primordia,
484   young fruiting body cap, gills and stipe, fruiting body cap and stipe were harvested for RNA
485   extraction. The hyphal knot stage was defined as an up to 0.5 mm diameter condensed hyphal
486   aggregate. Stage 1 primordia were defined as up to 2 mm tall shaft like structures, while stage 2
487   primordia up to 4 mm tall fruiting body initials with visible differentiation of cap and stipe initials.
488   Young fruiting bodies were up to 15 mm tall with a slightly elongated stipe and immature
489   basidia. Fruiting bodies had fully extended stipes and caps, being in an early autolytic phase.

490   Before fruiting, *Schizophyllum commune* the H4-8a and H4-8b monokaryons[4] were
491   grown on MM medium according to Dons et. al.[66]. After dikaryon formation an agar plug (5 mm)
492   was placed on the center of fresh MM medium at 30 °C for five days in the dark, then it was
493   placed at 25 °C for 10 days in a 12/12 hrs light/dark cycle (cool white F18w/840), upside down.
494   Dikaryotic vegetative mycelium, stage 1 and 2 primordia, young fruiting body and fruiting body
495   stages were harvested for RNA-seq. We defined stage 1 primordia as up to 2 mm fruiting body
496   initials, stage 2 primordia as 3-4 mm tall initials with an apical pit on the top, the young fruiting
497   body as a 5-7 mm tall cup-like structure with visible pseudolamellae inside, while fully expanded
498   ones were considered fruiting body.

499   Vegetative mycelia of *Lentinus tigrinus* RLP-9953-sp were maintained on MEA (20 g
500   malt extract, 0.5 g yeast extract, 15 g agar for 1L). For fruiting a mycelial plug was placed (5 mm
501   diameter) on modified sawdust-rice bran medium[67] (1 part wheat bran and 2 parts aspen
502   sawdust wetted to 65% moisture for 100 ml in a 250 ml beaker). The culture was incubated for
503   21 days at 30 °C in the dark, then placed in a moist growth chamber at 25 °C in a 12/12 hour
504   light/dark cycle. Vegetative mycelia, stage 1 primordia, stage 2 primordia cap and stipe, young
505   fruiting body cap and stipe and fruiting body cap and stipe tissues were harvested for RNA-Seq.
506   Stage 1 primordium was defined as a 5-20 mm tall white stalk-structure without any
507   differentiation of a cap initial, stage 2 primordium was defined as a 15 – 25 mm tall stalk-like
508   structure with a brown apical pigmentation (cap initial), young fruiting body had and up to 5 mm
509   wide brown cap initial with just barely visible gills on the bottom, growing on a 30-40 mm tall
510   stipe, fruiting body was 50-70 mm tall, with fully flattened (but not funnel-shaped) cap.

511   *Phanerochaete chrysosporium* RP-78 was fruited on YMPG media (10 g glucose, 10 g
512   malt extract, 2 g peptone, 2 g yeast extract, 1 g asparagine, 2 g KH_2PO_4, 1 g $MgSO_4$ x 7 H_2O,
513   20 g agar for 1L with 1 mg thiamine added after cooling) covered with cellophane for 7 days at
514   37 °C in the dark, then placed in a moist growth chamber at 25 °C in an area with dimmed
515   ambient light conditions, following the recommendations of Jill Gaskell (US Forest Products
516   Laboratory, Washington, D. C., USA). Vegetative mycelium, young fruiting body and fruiting

517 body stages were harvested for RNA extraction. Young fruiting body stage was defined as
518 fruiting body initials that forms a compact mat well-delimited from the surrounding vegetative
519 mycelium, while the fruiting bodies were harvested just after they started releasing spores
520 (visible on the lids of Petri dishes).
521 *Rickenella mellea* SZMC22713 was cultured on Fries Agar[68] for harvesting vegetative
522 mycelium for RNA and DNA extraction. DNA for genome sequencing was extracted using the
523 Blood & Cell Culture DNA Maxi Kit (Qiagen) from 300 mg finely ground mycelium powder
524 according to the manufacturer's instructions. The internal transcribed spacer region was PCR
525 amplified and sequenced to verify strain identity. For RNA-Seq, fruiting body stages were
526 collected in November 2016 from Kistelek, Hungary (approx. coordinates: 46.546309,
527 19.954507). Stage 1 primordium was defined as an approximately 1 mm tall, shaft-like, pear-
528 shaped structure, without any visible cap initial, stage 2 primordium was described as a 2-3 mm
529 tall structure with a small cap initial, young fruiting body was defined by the 5-15 mm tall
530 structure with a 1-2 mm wide cap, and the fruiting body was characterized by a fully expanded
531 cap on the top of a 20-32 mm tall stipe.
532 Data for *Armillaria ostoyae* C18/19 were taken from our previous study[16], with the
533 following stages defined: vegetative mycelium, stage 1 primordium, stage 2 primordium cap and
534 stipe, young fruiting body cap and stipe, and fruiting body cap, stipe and gills.
535 For RNA extraction all samples were immediately placed on liquid nitrogen after
536 harvesting and stored at -80 °C until use. Frozen tissues were weighed and 10-20 mg of *C.*
537 *cinerea, S. commune, P. chrysosporium* and *R. mellea* and 50-75 mg of *L. tigrinus* were
538 transferred to a pre-chilled mortar and ground to a fine powder using liquid nitrogen. We
539 extracted RNA of *C. cinerea, S. commune, P. chrysosporium* and *R. mellea* using the Quick-
540 RNA™ Miniprep (Zymo Research), or the RNeasy Midi Kit (QIAGEN) for *L. tigrinus.* Both of the
541 kits were used according to the manufacturer's instructions.
542

543 **De novo draft genome for *Rickenella mellea***
544 The genome and transcriptome of *Rickenella mellea* were sequenced using Illumina platform.
545 The genomes were sequenced as pairs of Illumina standard and Nextera long mate-pair (LMP)
546 libraries. For the Illumina Regular Fragment library, 100 ng of DNA was sheared to 300 bp using
547 the Covaris LE220 and size selected using SPRI beads (Beckman Coulter). The fragments
548 were treated with end-repair, A-tailing, and ligation of Illumina compatible adapters (IDT, Inc)
549 using the KAPA-Illumina library creation kit (KAPA biosystems).
550 For the Illumina Regular Long-mate Pair library (LMP), 5 ug of DNA was sheared using
551 the Covaris g-TUBE(TM) and gel size selected for 4 kb. The sheared DNA was treated with end
552 repair and ligated with biotinylated adapters containing *loxP*. The adapter ligated DNA
553 fragments were circularized via recombination by a Cre excision reaction (NEB). The
554 circularized DNA templates were then randomly sheared using the Covaris LE220 (Covaris).
555 The sheared fragments were treated with end repair and A-tailing using the KAPA-Illumina
556 library creation kit (KAPA biosystems) followed by immobilization of mate pair fragments on
557 streptavidin beads (Invitrogen). Illumina compatible adapters (IDT, Inc) were ligated to the mate
558 pair fragments and 8 cycles of PCR was used to enrich for the final library (KAPA Biosystems).
559 Stranded cDNA libraries were generated using the Illumina Truseq Stranded RNA LT kit.
560 mRNA was purified from 1 µg of total RNA using magnetic beads containing poly-T oligos.

561 mRNA was fragmented and reversed transcribed using random hexamers and SSII (Invitrogen)
562 followed by second strand synthesis. The fragmented cDNA was treated with end-pair, A-tailing,
563 adapter ligation, and 8 cycles of PCR.
564   The prepared libraries were quantified using KAPA Biosystem's next-generation
565 sequencing library qPCR kit and run on a Roche LightCycler 480 real-time PCR instrument. The
566 quantified libraries were then multiplexed with other libraries, and the pool of libraries was then
567 prepared for sequencing on the Illumina HiSeq sequencing platform utilizing a TruSeq paired-
568 end cluster kit, v4, and Illumina's cBot instrument to generate a clustered flow cell for
569 sequencing. Sequencing of the flow cell was performed on the Illumina HiSeq2500 sequencer
570 using HiSeq TruSeq SBS sequencing kits, v4, following a 2x150 indexed run recipe (2x100bp
571 for LMP).
572   Genomic reads from both libraries were QC filtered for artifact/process contamination
573 and assembled together with AllPathsLG v. R49403[69]. Illumina reads of stranded RNA-seq data
574 were used as input for de novo assembly of RNA contigs, assembled into consensus
575 sequences using Rnnotator (v. 3.4)[70]. Both genomes were annotated using the JGI Annotation
576 Pipeline and made available via the JGI fungal portal MycoCosm[71]. Genome assemblies and
577 annotation were also deposited at DDBJ/EMBL/GenBank under the accession XXXXX (TO BE
578 PROVIDED UPON PUBLICATION).
579
580 **RNA-Seq**
581 Whole transcriptome sequencing was performed using the TrueSeq RNA Library Preparation Kit
582 v2 (Illumina) according to the manufacturer's instructions. Briefly, RNA quality and quantity
583 measurements were performed using RNA ScreenTape and Reagents on TapeStation (all from
584 Agilent) and Qubit (ThermoFisher); only high quality (RIN >8.0) total RNA samples were
585 processed. Next, RNA was DNaseI (ThermoFisher) treated and the mRNA was purified and
586 fragmented. First strand cDNA synthesis was performed using SuperScript II (ThermoFisher)
587 followed by second strand cDNA synthesis, end repair, 3'-end adenylation, adapter ligation and
588 PCR amplification. All of the purification steps were performed using AmPureXP Beads
589 (Backman Coulter). Final libraries were quality checked using D1000 ScreenTape and
590 Reagents on TapeStation (all from Agilent). Concentration of each library was determined using
591 either the QPCR Quantification Kit for Illumina (Agilent) or the KAPA Library Quantification Kit
592 for Illumina (KAPA Biosystems). Sequencing was performed on Illumina instruments using the
593 HiSeq SBS Kit v4 250 cycles kit (Illumina) or the NextSeq 500/550 High Output Kit v2 300
594 cycles (Illumina) generating >20 million clusters for each sample.
595
596 **Bioinformatic analyses of RNA-Seq data**
597 RNA-Seq analyses were carried out as reported earlier[16]. Paired-end Illumina (HiSeq, NextSeq)
598 reads were quality trimmed using the CLC Genomics Workbench tool version 9.5.2 (CLC
599 Bio/Qiagen) removing ambiguous nucleotides as well as any low quality read end parts. Quality
600 cutoff value (error probability) was set to 0.05, corresponding to a Phred score of 13. Trimmed
601 reads containing at least 40 bases were mapped using the RNA-Seq Analysis 2.1 package in
602 CLC requiring at least 80% sequence identity over at least 80% of the read lengths; strand
603 specificity was omitted. List of reference sequences is provided as Supplementary table 1.
604 Reads with less than 30 equally scoring mapping positions were mapped to all possible

605   locations while reads with more than 30 potential mapping positions were considered as
606   uninformative repeat reads and were removed from the analysis.
607   "Total gene read" RNA-Seq count data was imported from CLC into R version 3.0.2.
608   Genes were filtered based on their expression levels keeping only those features that were
609   detected by at least five mapped reads in at least 25% of the samples included in the study.
610   Subsequently, "calcNormFactors" from "edgeR" version 3.4.2[72] was used to perform data
611   scaling based on the "trimmed mean of M-values" (TMM) method[73]. Log transformation was
612   carried out by the "voom" function of the "limma" package version 3.18.13[74]. Linear modeling,
613   empirical Bayes moderation as well as the calculation of differentially expressed genes were
614   carried out using "limma". Genes showing at least four-fold gene expression change with an
615   FDR value below 0.05 were considered as significant. Multi-dimensional scaling ("plotMDS"
616   function in edgeR) was applied to visually summarize gene expression profiles revealing
617   similarities between samples. In addition, unsupervised cluster analysis with Euclidean distance
618   calculation and complete-linkage clustering was carried out on the normalized data using
619   "heatmap.2" function from R package "gplots".
620

621   **Identification of developmentally regulated genes**
622   We considered genes with a Fragments Per Kilobase Million (FPKM) value >1 to have a non-
623   zero expression. Because differentially expressed genes can only be defined in pairwise
624   comparisons of samples and thus didn't suit our developmental series data, we opted to use the
625   concept of developmentally regulated gene. These were defined as any gene showing an over
626   four-fold change in expression between any two developmental stages or tissue types and a
627   maximum expression level of FPKM > 4 in at least one developmental stage. Comparisons
628   between tissue types were only performed within the respective developmental stage. We
629   distinguished developmentally regulated genes that showed over four-fold upregulation at
630   fruiting body initiation ('FB-init' genes) and those that show over four-fold expression dynamics
631   (up- or downregulation) across the range of fruiting body stages ('FB genes', i.e. vegetative
632   mycelium excluded). Note that this strategy excludes genes showing highest expression in
633   vegetative mycelium and no dynamics later on, to remove genes with a significant
634   downregulation at the onset of fruiting body development (e.g. those involved in nutrient
635   acquisition by the mycelium).
636

637   **Comparative genomic approaches**
638   To obtain characteristic Interpro domain signatures of Agaricomycetes, we assembled a dataset
639   comprising genomes of 201 species; ranging from simple unicellular yeasts to filamentous and
640   complex multicellular fungi. InterProscan version 5.24-63.0 was used to perform IPR searches.
641   The 201 species were categorized into two major groups; mushroom-forming fungi (113
642   species) and all other fungi (88 species, 1 Cryptomycota, 2 Microsporidia, 2
643   Neocallimastigomycota, 3 Chytridiomycota, 2 Blastocladiomycota, 14 Zygomycota, 1
644   Glomeromycota, 38 Ascomycota, 20 non-fruiting body forming Basidiomycota). The enrichment
645   of IPR domains was tested using Fisher's exact test and corrected for multiple testing by the
646   Benjamini-Hochberg method in R (R core team 2016). P<0.01 was considered significant.
647   Significantly overrepresented IPR domains were characterized by Gene Ontology Terms using
648   IPR2GO.

649   An all-versus-all protein BLAST was performed for the six species (*A. ostoyae, C.*
650   *cinerea, S. commune, L. tigrinus, P. chrysosporium, R. mellea*) and for the 201-species dataset
651   using mpiBLAST (v.1.6.0) with default parameters. Clustering was done using Markov Cluster
652   with an inflation parameter of 2.0[25].

653

654   **Reconstruction of alternative splicing patterns**
655   We reconstructed patterns of alternative splicing using the RNA-Seq data for all six species. To
656   this end, we used region-restricted probabilistic modelling (RRPM)[21] to discover alternative
657   transcripts, as described by Gehrmann et al.. Briefly, the genome was split at gene boundaries
658   into fragments, then all RNA-Seq reads were aligned to these fragments with STAR v2.5.3a[75], in
659   two rounds. The first round of read alignment was run to produce a novel splice junction
660   database, which was used to improve mapping in the second round. Using the BAM file from
661   this alignment, Cufflinks v2.2.1[76] was run in RABT mode to predict novel transcripts. To restore
662   the context, these sets of transcripts were projected back onto the original annotation. The
663   resulting annotation file was filtered to remove predicted transcripts with no detectable
664   expression (FPKM = 0) or did not have reads supporting its splice junctions. We performed read
665   alignment using STAR again with the same two round method and the new, corrected
666   annotation file and used the Cufflinks suite to estimate the expression level for each transcript.
667   We then aligned reads of each RNA-Seq replicate separately to the genome with updated gene
668   annotation. This resulted in an expression profile for each alternatively spliced transcript, in
669   every developmental stage. We subsequently identified developmentally regulated transcripts
670   using the same functions as described above for genes. For splicing event discovery, we used
671   the ASpli[77] R package where we used the most significant transcript (the most abundant
672   transcript through the developmental stages) as the reference for event discovery. Custom
673   scripts were used to extract stage and tissue-type specificity and distribution of spliced genes
674   and splicing events.

675

676   **Phylostratigraphic analysis**
677   To examine the evolutionary origin of developmentally regulated genes in each species, a
678   phylostatigraphic analysis was performed[19]. First, we assembled a database containing
679   genomes covering the evolutionary route from the most recent common ancestor of cellular
680   organisms to the respective species, by complementing the database of Drost et al.[20]. Fungal,
681   microsporidia and plant genomes were removed from this database and substituted by 416
682   fungal genomes (all published), including 382 belonging to the Dikarya and 116 to the
683   Agaricomycetes. In addition, 6 microsporidia, 59 plant and 6 Opisthokonta[78] genomes were
684   added, resulting in a database of 4,483 genomes. The database was divided into age
685   categories ('phylostrata') based on the tree available at Mycocosm[71] and the eukaryotic tree
686   published by Torruella et al.[78]. The oldest phylostratum consisted of bacteria and archaea.
687   Whole proteomes of *Coprinopsis cinerea*, *Armillaria ostoyae*, *Schizophyllum commune*,
688   *Lentinus tigrinus*, *Phanerochaete chrysosporium* and *Rickenella mellea* were blasted against
689   this database using mpiblast 1.6.0[79] with default settings. Blast hits were filtered with an E-value
690   cut-off of 1×10^{-6} and a query coverage cut-off of 80%. After filtering, the age of each gene was

19

691   defined as the node of the tree representing the last common ancestor of the species sharing
692   homologs of the gene, at the specified blast cutoff.
693   To infer what Agaricomycete-specific genes are preferentially developmentally
694   regulated, we analyzed the enrichment of annotation terms among developmentally regulated
695   genes specific to Agaricomycetes compared to developmentally regulated genes whose origin
696   predates the Agaricomycetes. To this end, we divided the phylostratigraphy profiles into two
697   groups, corresponding to genes that originated before and those that originated after the origin
698   of mushroom-forming fungi (Phylostratum 18). We tested for significant enrichment of IPR
699   domains (evalue < 1e-5) in developmentally regulated genes that originated within the
700   Agaricomycetes, relative to the other group of more ancient developmentally regulated genes
701   using Fisher's exact test (P < 0.05).
702

703   **CAZyme annotation**
704   Genes encoding putative carbohydrate-active enzymes were annotated using the CAZy
705   pipeline. BLAST and Hmmer searches were conducted against sequence libraries and HMM
706   profiles in the CAZy database[80] (http://www.cazy.org). Positive hits were validated manually and
707   assigned a family and subfamily classification across Glycoside Hydrolase (GH), Carbohydrate
708   Esterase (CE), Glycoside Transferase (GT), Polysaccharide Lyase (PL), Carbohydrate-Binding
709   Module (CBM) and Auxiliary redox enzyme (AA) classes of the CAZy system[81]. Activities were
710   determined by BLAST searches against biochemically characterized subsets of the CAZy
711   database.
712

713   **Coexpression analysis**
714   Developmentally regulated genes in each species were clustered into co-expression modules
715   based on their expression dynamics by using the clustering method implemented in Short Time-
716   series Expression Miner (STEM v. 1.3.11)[18,82]. Default parameters were used, except minimum
717   absolute expression change, which was set to 4. Functional annotations of modules were
718   obtained by GO enrichment analyses in TopGO (see below). For a higher-level grouping of co-
719   expression modules, we defined six categories corresponding to early and late expressed
720   genes, cap, stipe and gill specific genes and a mixed category. Coexpression modules were
721   placed in one of these categories if more than half of the module's members had the same
722   tissue- or stage-specific expression peaks. Modules without stage or tissue specificity were
723   grouped in the mixed category. The early expressed category included coexpression modules
724   with expression peaks in H, P1 or P2 stages, while late module category consisted of modules
725   with young fruiting body and fruiting body stage specific expression peaks. We functionally
726   annotated the modules and higher categories using InterPro Scan v5.24-63.0.
727   To visualize the kinase expression network across various kinase groups and
728   developmental stages, a co-expression network was visualized using Cytoscape *v*3.6.1 based
729   on pairwise Pearson correlation coefficients for kinase expression patterns in *Coprinopsis*
730   *cinerea*. Pairwise Pearson correlations coefficients for each kinase gene pair were calculated
731   and a 0.85 cut-off was applied for network construction.
732

733   **Functional annotations, GO and Interpro enrichment**

734   Gene Ontology (GO) enrichment analyses were carried out for developmentally regulated
735   genes. For this, we annotated genes with GO terms based on their InterPro domain contents.
736   Analyses were performed using Fisher's exact test with threshold P<0.05 in the R package
737   topGO. The parameter algorithm weighted01 was chosen. Heatmaps were created using the
738   heatmap.2 function of the R package 'gplots'. Unsupervised cluster analysis with Pearson's
739   distance calculation and averaged-linkage clustering was carried out on the FPKM values, and
740   heatmaps was visualised using z-score normalization on the rows via the heatmap.2 function.

741   Prediction of glycosylphosphatidylinositol anchored proteins (GPI-Ap) for the six species
742   was performed using the portable version of Pred-GPI[83]. From the proteins with a predicted
743   GPI-anchor, we excluded ones which had no extracellular signal sequence, as assessed by
744   SignalP version 4.1[84]. Prediction of Small Secreted Proteins (SSP) for the six species was
745   performed using a modified version of the bioinformatic pipeline of Pellegrin et al.[44]. Proteins
746   shorter than 300 amino acids were subjected to signal peptide prediction in SignalP (version
747   4.1) with the option "eukaryotic". Extracellular localisation of these proteins was checked with
748   WoLFPsort version 0.2[85] using the option "fungi". Proteins containing transmembrane helix not
749   overlapping with the signal peptide were also excluded. Prediction of transmembrane helices
750   was performed with TMHMM (version 2.0)[86]. Finally, proteins containing a KDEL motif (Lys-Asp-
751   Glu-Leu) in the C-terminal region (prosite accession "PS00014") responsible for retention in the
752   endoplasmic reticulum (ER) lumen, were identified using PS-SCAN (http://www.hpa-
753   bioinfotools.org.uk/cgi-bin/ps_scan/ps_scanCGI.pl) and excluded.

754   We identified transcription factors based on the presence of InterPro domains with
755   sequence-specific DNA-binding activity retrieved from literature data[87,88] and manual curation of
756   the Interpro-database. Annotated genes were then filtered based on their domain architecture in
757   order to discard genes encoding DNA-binding proteins with functions other than transcription
758   regulation (such as DNA-repair, DNA-replication, translation, meiosis).

759   We extracted the putative kinase genes from the 6 species based on their InterPro
760   domain composition, and manually curated the classical kinases by excluding domains which
761   correspond to metabolism related kinases and other non-classical protein kinases. The set of
762   proteins having kinase related domains (Supplementary table 12) were subjected to BLAST
763   searches (*BLAST 2.7.1+*, E-value 0.001) against the kinome of *Coprinopsis cinerea*[3]
764   downloaded from Kinbase (www.kinase.com). The best hits for the six species were classified
765   into eukaryotic protein kinase (ePK) and atypical protein kinases (aPK) and their families and
766   subfamilies as described in the hierarchical kinase classification system[54].

Acknowledgements

Author contributions

K.K. and L.G.N. conceived the study. K.K., B.K., E.A. performed fruiting experiments, RNA isolation and data analysis. B.B., I.N., J.C. obtained and analysed RNA-Seq data. Z.M., N.S., M.V., T.K. and L.G.N. performed comparative genomic and phylogenomic analyses. S.M. analyzed the genomic context of F-box gene duplications. B.H. analyzed CAZymes. E.A. and R.A.O. analyzed transcription factors. B.H. contributed valuable analytical insights. K.B., J.J., A.L., J.P., J.Y. Y.X. and I.V.G. sequences, assembled and annotated the genome of *Rickenella mellea*. L.G.N, K.K., B.B., and U.K. wrote the manuscript. D.S.H. contributed the genome of *Lentinus tigrinus* and analytical insights. All authors read and commented on the manuscript.

Data availability

Genome assembly and annotation of *Rickenella mellea* was deposited at DDBJ/ EMBL/GenBank under the accession XXXXXX (to be provided upon publication). A Gene Expression Omnibus (GEO) archive of the sequenced *A. ostoyae* libraries was deposited in the NCBI's GEO Archive at http://www.ncbi.nlm.nih.gov/geo under accession SRP109671.

References

1. Kohler, A. *et al.* Convergent losses of decay mechanisms and rapid turnover of symbiosys genes in mycorrhizal mutualists. *Nat. Genet.* **47,** 410-415**,** (2015).
2. Kalaras, M. D., Richie, J. P., Calcagnotto, A. & Beelman, R. B. Mushrooms: A rich source of the antioxidants ergothioneine and glutathione. *Food Chem.* **233,** 429–433 (2017).
3. Stajich, J. E. *et al.* Insights into evolution of multicellular fungi from the assembled chromosomes of the mushroom Coprinopsis cinerea (Coprinus cinereus). *Proc Natl Acad Sci U S A* **107,** 11889–11894 (2010).
4. Ohm, R. A. *et al.* Genome sequence of the model mushroom Schizophyllum commune. *Nat. Biotechnol.* **28,** 957–963 (2010).
5. Kues, U. Life history and developmental processes in the basidiomycete Coprinus cinereus. *Microbiol Mol Biol Rev* **64,** 316–353 (2000).
6. Kües, U. & Navarro-González, M. How do Agaricomycetes shape their fruiting bodies? 1. Morphological aspects of development. *Fungal Biology Reviews* **29,** 63–97 (2015).
7. Nagy, L. G., Kovács, G. M. & Krizsán, K. Complex multicellularity in fungi: evolutionary convergence, single origin, or both? *Biol. Rev.* (2018). doi:10.1111/brv.12418
8. Bayry, J., Aimanianda, V., Guijarro, J. I., Sunde, M. & Latgé, J. P. Hydrophobins-unique fungal proteins. *PLoS Pathog.* **8,** (2012).
9. Plaza, D. F., Lin, C. W., van der Velden, N. S., Aebi, M. & Kunzler, M. Comparative transcriptomics of the model mushroom Coprinopsis cinerea reveals tissue-specific armories and a conserved circuitry for sexual development. *BMC Genomics* **15,** 492 (2014).
10. Buser, R., Lazar, Z., Käser, S., Künzler, M. & Aebi, M. Identification, characterization, and biosynthesis of a novel N-glycan modification in the fruiting body of the basidiomycete Coprinopsis cinerea. *J. Biol. Chem.* **285,** 10715–10723 (2010).
11. Ohga, S., Cho, N.-S., Thurston, C. F. & Wood, D. A. Transcriptional regulation of laccase and cellulase in relation to fruit body formation in the mycelium of Lentinula edodes on a sawdust-based substrate. *Mycoscience* **41,** 149–153 (2000).
12. Konno, N. & Sakamoto, Y. An endo-$β$-1,6-glucanase involved in Lentinula edodes fruiting body autolysis. *Appl. Microbiol. Biotechnol.* **91,** 1365–1373 (2011).
13. Sakamoto, Y. *et al.* Lentinula edodes tlg1 encodes a thaumatin-like protein that is

822   involved in lentinan degradation and fruiting body senescence. *Plant Physiol.* **141,** 793–
823   801 (2006).
824 14. Ohm, R. A., de Jong, J. F., de Bekker, C., Wösten, H. A. B. & Lugones, L. G.
825   Transcription factor genes of Schizophyllum commune involved in regulation of
826   mushroom formation. *Mol. Microbiol.* **81,** 1433–1445 (2011).
827 15. Corrochano, L. M. Fungal photoreceptors: sensory molecules for fungal development and
828   behaviour. *Photochem. Photobiol. Sci.* **6,** 725 (2007).
829 16. Sipos, G. *et al.* Genome expansion and lineage-specific genetic innovations in the forest
830   pathogenic fungi Armillaria. *Nat. Ecol. Evol.* **1,** 1931–1941 (2017).
831 17. Clémençon, H., Emmett, V. & Emmett, E. E. *Cytology and plectology of the
832   Hymenomycetes with 12 tables.* (Cramer in der Gebr.-Borntraeger-Verl.-Buchh, 2012).
833 18. Ernst, J. & Bar-Joseph, Z. STEM: A tool for the analysis of short time series gene
834   expression data. *BMC Bioinformatics* **7,** (2006).
835 19. Domazet-Lošo, T., Brajković, J. & Tautz, D. A phylostratigraphy approach to uncover the
836   genomic history of major adaptations in metazoan lineages. *Trends in Genetics* **23,** 533–
837   539 (2007).
838 20. Drost, H. G., Gabel, A., Grosse, I. & Quint, M. Evidence for active maintenance of
839   phylotranscriptomic hourglass patterns in animal and plant embryogenesis. *Mol. Biol.
840   Evol.* **32,** 1221–1231 (2015).
841 21. Gehrmann, T. *et al.* Schizophyllum commune has an extensive and functional alternative
842   splicing repertoire. *Sci. Rep.* **6,** (2016).
843 22. Xie, B.-B. *et al.* Deep RNA sequencing reveals a high frequency of alternative splicing
844   events in the fungus Trichoderma longibrachiatum. *BMC Genomics* **16,** 54 (2015).
845 23. Wang, B. *et al.* Survey of the transcriptome of Aspergillus oryzae via massively parallel
846   mRNA sequencing. *Nucleic Acids Res.* **38,** 5075–5087 (2010).
847 24. Gordon, S. P. *et al.* Widespread polycistronic transcripts in fungi revealed by single-
848   molecule mRNA sequencing. *PLoS One* **10,** (2015).
849 25. Enright, A. J., Van Dongen, S. & Ouzounis, C. A. An efficient algorithm for large-scale
850   detection of protein families. *Nucleic Acids Res.* **30,** 1575–1584 (2002).
851 26. Sakamoto, Y., Nakade, K. & Konno, N. Endo-$β$-1,3-Glucanase GLU1, from the fruiting
852   body of Lentinula edodes, belongs to a new glycoside hydrolase family. *Appl. Environ.
853   Microbiol.* **77,** 8350–8354 (2011).
854 27. Fukuda, K. *et al.* Purification and characterization of a novel exo-beta-1,3-1,6-glucanase
855   from the fruiting body of the edible mushroom Enoki (Flammulina velutipes). *Biosci.
856   Biotechnol. Biochem.* **72,** 3107–3113 (2008).
857 28. Zhou, Y., Zhang, W., Liu, Z., Wang, J. & Yuan, S. Purification, characterization and
858   synergism in autolysis of a group of 1,3-$β$-glucan hydrolases from the pilei of
859   Coprinopsis cinerea fruiting bodies. *Microbiol. (United Kingdom)* **161,** 1978–1989 (2015).
860 29. Szeto, C. Y., Leung, G. S. & Kwan, H. S. Le.MAPK and its interacting partner, Le.DRMIP,
861   in fruiting body development in Lentinula edodes. *Gene* **393,** 87–93 (2007).
862 30. Kersten, P. & Cullen, D. Copper radical oxidases and related extracellular
863   oxidoreductases of wood-decay Agaricomycetes. *Fungal Genet. Biol.* **72,** 124–130
864   (2014).
865 31. Rytioja, J. *et al.* Plant-Polysaccharide-Degrading Enzymes from Basidiomycetes.
866   *Microbiol. Mol. Biol. Rev.* **78,** 614–649 (2014).
867 32. Tovar-Herrera, O. E. *et al.* A novel expansin protein from the white-rot fungus
868   Schizophyllum commune. *PLoS One* **10,** (2015).
869 33. Lenfant, N. *et al.* A bioinformatics analysis of 3400 lytic polysaccharide oxidases from
870   family AA9. *Carbohydr. Res.* **448,** 166–174 (2017).
871 34. Temp, U. & Eggert, C. Novel interaction between laccase and cellobiose dehydrogenase
872   during pigment synthesis in the white rot fungus Pycnoporus cinnabarinus. *Appl. Environ.*

873   *Microbiol.* **65,** 389–395 (1999).

874   35.   Osińska-Jaroszuk, M. *et al.* Complex biochemical analysis of fruiting bodies from newly
875   isolated polish Flammulina velutipes strains. *Polish J. Microbiol.* **65,** 295–305 (2016).

876   36.   Ji, J. & Moore, D. Glycogen metabolism in relation to fruit body maturation in Coprinus
877   cinereus. *Mycol. Res.* **97,** 283–289 (1993).

878   37.   Dranginis, A. M., Rauceo, J. M., Coronado, J. E. & Lipke, P. N. A Biochemical Guide to
879   Yeast Adhesins: Glycoproteins for Social and Antisocial Occasions. *Microbiol. Mol. Biol.*
880   *Rev.* **71,** 282–294 (2007).

881   38.   Lugones, L. G. *et al.* Hydrophobins line air channels in fruiting bodies of Schizophyllum
882   commune and Agaricus bisporus. *Mycol. Res.* **103,** 635–640 (1999).

883   39.   Gaderer, R., Bonazza, K. & Seidl-Seiboth, V. Cerato-platanins: A fungal protein family
884   with intriguing properties and application potential. *Applied Microbiology and*
885   *Biotechnology* **98,** 4795–4803 (2014).

886   40.   Martin, F., Kohler, A., Murat, C., Veneault-Fourrey, C. & Hibbett, D. S. Unearthing the
887   roots of ectomycorrhizal symbioses. *Nat. Rev. Microbiol.* **14,** 760–773 (2016).

888   41.   Stergiopoulos, I. & de Wit, P. J. G. M. Fungal Effector Proteins. *Annu. Rev. Phytopathol.*
889   **47,** 233–263 (2009).

890   42.   Feldman, D., Kowbel, D. J., Glass, N. L., Yarden, O. & Hadar, Y. A role for small secreted
891   proteins (SSPs) in a saprophytic fungal lifestyle: Ligninolytic enzyme regulation in
892   Pleurotus ostreatus. *Sci. Rep.* **7,** (2017).

893   43.   Wang, L., Tian, X., Gyawali, R. & Lin, X. Fungal adhesion protein guides community
894   behaviors and autoinduction in a paracrine manner. *Proc Natl Acad Sci U S A* **110,**
895   11571–11576 (2013).

896   44.   Pellegrin, C., Morin, E., Martin, F. M. & Veneault-Fourrey, C. Comparative Analysis of
897   Secretomes from Ectomycorrhizal Fungi with an Emphasis on Small-Secreted Proteins.
898   *Front. Microbiol.* **6,** 1278 (2015).

899   45.   Liu, T. B. & Xue, C. The ubiquitin-proteasome system and F-box proteins in pathogenic
900   fungi. *Mycobiology* **39,** 243–248 (2011).

901   46.   Xu, G., Ma, H., Nei, M. & Kong, H. Evolution of F-box genes in plants: Different modes of
902   sequence divergence and their relationships with functional diversification. *Proc. Natl.*
903   *Acad. Sci.* **106,** 835–840 (2009).

904   47.   Metzger, M. B., Pruneda, J. N., Klevit, R. E. & Weissman, A. M. RING-type E3 ligases:
905   Master manipulators of E2 ubiquitin-conjugating enzymes and ubiquitination. *Biochimica*
906   *et Biophysica Acta - Molecular Cell Research* **1843,** 47–60 (2014).

907   48.   Chae, E., Tan, Q. K.-G., Hill, T. A. & Irish, V. F. An Arabidopsis F-box protein acts as a
908   transcriptional co-factor to regulate floral development. *Development* **135,** 1235–1245
909   (2008).

910   49.   Pöggeler, S., Nowrousian, M., Teichert, I., Beier, A. & Kück, U. Fruiting-Body
911   Development in Ascomycetes. in *Physiology and Genetics* 1–56 (Springer International
912   Publishing, 2018). doi:10.1007/978-3-319-71740-1_1

913   50.   Dharmasiri, N. *et al.* Plant Development Is Regulated by a Family of Auxin Receptor F
914   Box Proteins. *Dev. Cell* **9,** 109–119 (2005).

915   51.   Pelkmans, J. F. *et al.* The transcriptional regulator c2h2 accelerates mushroom formation
916   in Agaricus bisporus. *Appl. Microbiol. Biotechnol.* **100,** 7151–7159 (2016).

917   52.   Muraguchi, H. *et al.* Strand-specific RNA-seq analyses of fruiting body development in
918   Coprinopsis cinerea. *PLoS One* **10,** (2015).

919   53.   Pelkmans, J. F. *et al.* Transcription factors of schizophyllum commune involved in
920   mushroom formation and modulation of vegetative growth. *Sci. Rep.* **7,** (2017).

921   54.   Manning, G., Whyte, D. B., Martinez, R., Hunter, T. & Sudarsanam, S. The protein kinase
922   complement of the human genome. *Science* **298,** 1912–1934 (2002).

923   55.   Kosti, I., Mandel-Gutfreund, Y., Glaser, F. & Horwitz, B. A. Comparative analysis of fungal

924   protein kinases and associated domains. *BMC Genomics* **11,** (2010).

925 56. Zhao, Z., Jin, Q., Xu, J. R. & Liu, H. Identification of a fungi-specific lineage of protein
926   kinases closely related to tyrosine kinases. *PLoS One* **9,** (2014).

927 57. Lehti-Shiu, M. D. & Shiu, S.-H. Diversity, classification and function of the plant protein
928   kinase superfamily. *Philos. Trans. R. Soc. B Biol. Sci.* **367,** 2619–2639 (2012).

929 58. Knoll, A. H. The Multiple Origins of Complex Multicellularity. *Earth Planet. Sci.* **39,** 217–
930   239 (2011).

931 59. Shiu, S. H. & Bleecker, a B. Plant receptor-like kinase gene family: diversity, function,
932   and signaling. *Sci. STKE* **2001,** re22 (2001).

933 60. Kunzler, M. Hitting the sweet spot-glycans as targets of fungal defense effector proteins.
934   *Molecules* **20,** 8144–8167 (2015).

935 61. Schubert, M. *et al.* Plasticity of the β-trefoil protein fold in the recognition and control of
936   invertebrate predators and parasites by a fungal defence system. *PLoS Pathog.* **8,**
937   (2012).

938 62. Cock, J. M. *et al.* The Ectocarpus genome and the independent evolution of
939   multicellularity in brown algae. *Nature* **465,** 617–621 (2010).

940 63. Sebe-Pedros, A., Degnan, B. M. & Ruiz-Trillo, I. The origin of Metazoa: a unicellular
941   perspective. *Nat Rev Genet* **18,** 498–512 (2017).

942 64. Nguyen, T. A. *et al.* Innovation and constraint leading to complex multicellularity in the
943   Ascomycota. *Nat Commun* **8,** 14444 (2017).

944 65. Granado, J. D., Kertesz-Chaloupková, K., Aebi, M. & Kües, U. Restriction enzyme-
945   mediated DNA integration in Coprinus cinereus. *Mol. Gen. Genet. MGG* **256,** 28–36
946   (1997).

947 66. Dons, J. J. M., De Vries, O. M. H. & Wessels, J. G. H. Characterization of the genome of
948   the basidiomycete Schizophyllum commune. *BBA Sect. Nucleic Acids Protein Synth.* **563,**
949   100–112 (1979).

950 67. Hibbett, D. S., Murakami, S. & Tsuneda, A. Hymenophore Development and Evolution in
951   Lentinus. *Mycologia* **85,** 428 (1993).

952 68. Fries, N. Basidiospore germination in some mycorrhiza-forming hymenomycetes. *Trans.*
953   *Br. Mycol. Soc.* **70,** 319–324 (1978).

954 69. Gnerre, S. *et al.* High-quality draft assemblies of mammalian genomes from massively
955   parallel sequence data. *Proc. Natl. Acad. Sci.* **108,** 1513–1518 (2011).

956 70. Martin, J. *et al.* Rnnotator: An automated de novo transcriptome assembly pipeline from
957   stranded RNA-Seq reads. *BMC Genomics* **11,** (2010).

958 71. Grigoriev, I. V *et al.* MycoCosm portal: Gearing up for 1000 fungal genomes. *Nucleic*
959   *Acids Res.* **42,** (2014).

960 72. Robinson, M. D., McCarthy, D. J. & Smyth, G. K. edgeR: a Bioconductor package for
961   differential expression analysis of digital gene expression data. *Bioinformatics* **26,** 139–
962   140 (2010).

963 73. Robinson, M. D. & Oshlack, A. A scaling normalization method for differential expression
964   analysis of RNA-seq data. *Genome Biol.* **11,** (2010).

965 74. Ritchie, M. E. *et al.* Limma powers differential expression analyses for RNA-sequencing
966   and microarray studies. *Nucleic Acids Res.* **43,** e47 (2015).

967 75. Dobin, A. *et al.* STAR: Ultrafast universal RNA-seq aligner. *Bioinformatics* **29,** 15–21
968   (2013).

969 76. Trapnell, C. *et al.* Transcript assembly and quantification by RNA-Seq reveals
970   unannotated transcripts and isoform switching during cell differentiation. *Nat. Biotechnol.*
971   **28,** 511–515 (2010).

972 77. Mancini, E., Iserte, J., Yanocsky, M. & Chernomoretz, A. ASpli: An integrative R package
973   for analysing alternative splicing using RNAseq - Semantic Scholar. (2017).

974 78. Torruella, G. *et al.* Phylogenomics Reveals Convergent Evolution of Lifestyles in Close

975   Relatives of Animals and Fungi. *Curr. Biol.* **25,** 2404–2410 (2015).

976 79. Darling, A. E., Carey, L. & Feng, W.-C. The Design, Implementation, and Evaluation of
977   mpiBLAST. in *ClusterWorld Conference & Expo and the 4th International Conference on*
978   *Linux Clusters: The HPC Revolution* (2003).

979 80. Lombard, V., Golaconda Ramulu, H., Drula, E., Coutinho, P. M. & Henrissat, B. The
980   carbohydrate-active enzymes database (CAZy) in 2013. *Nucleic Acids Res.* **42,** (2014).

981 81. Levasseur, A., Drula, E., Lombard, V., Coutinho, P. M. & Henrissat, B. Expansion of the
982   enzymatic repertoire of the CAZy database to integrate auxiliary redox enzymes.
983   *Biotechnol. Biofuels* **6,** (2013).

984 82. Ernst, J., Nau, G. J. & Bar-Joseph, Z. Clustering short time series gene expression data.
985   *Bioinformatics* **21,** (2005).

986 83. Pierleoni, A., Martelli, P. & Casadio, R. PredGPI: a GPI-anchor predictor. *BMC*
987   *Bioinformatics* **9,** 392 (2008).

988 84. Petersen, T. N., Brunak, S., Von Heijne, G. & Nielsen, H. SignalP 4.0: Discriminating
989   signal peptides from transmembrane regions. *Nature Methods* **8,** 785–786 (2011).

990 85. Horton, P. *et al.* WoLF PSORT: Protein localization predictor. *Nucleic Acids Res.* **35,**
991   (2007).

992 86. Melén, K., Krogh, A. & Von Heijne, G. Reliability measures for membrane protein
993   topology prediction algorithms. *J. Mol. Biol.* **327,** 735–744 (2003).

994 87. Shelest, E. Transcription Factors in Fungi: TFome Dynamics, Three Major Families, and
995   Dual-Specificity TFs. *Front. Genet.* **8,** 53 (2017).

996 88. Chen, L. *et al.* Genome Sequence of the Edible Cultivated Mushroom Lentinula edodes
997   (Shiitake) Reveals Insights into Lignocellulose Degradation. *PLoS One* **11,** e0160336
998   (2016).

999
1000

1001 ## Tables

1002 **Table 1 Conserved developmentally regulated (CAZyme) families and associated modules**

Family	Activity	Putative FCW role/substrate	Conservation	Reports of role in development	Expansion in Agaricomycetes
AA1_1	Laccase	crosslinking	5 (P.chr.)	Several reports	7.2×10^{-90}
AA3_1	Cellobiose dehydrogenase	chitin	5 (L.tig)	Temp&Eggert 1990	9.6×10^{-56}
AA3_2/3	Glucose oxidase, aryl alcohol oxidase	H_2O_2 generation, light recetor?	6	This study	$<10^{-300}$
AA5_1/2	Glyoxal oxidase, galactose oxidase	H_2O_2 generation	6	This study	2.2×10^{-3}
AA9	Lytic polysaccharide monooxygenase	chitin	6	This study	5.6×10^{-86}
CBM1	cellulose/chitin binding	chitin	5 (S.com.)	This study	n.s.
CBM12	Chitin binding	chitin	5 (P.chr.)	Sakamoto et al 2017	n.s.
CBM50	Chitin binding	chitin	5 (S.com.)	This study	1.7×10^{-51}
CE4	chitooligosaccharide deacetylase	Chitin / chitosan	6	This study	6.4×10^{-11}
CE8	Pectin methylesterase	unknown	5 (C.cin.)	This study	n.s.
GH1_4	β-glucosidase	glucan	6	This study	n.s.
GH3_5	exo-β-1,3-glucanase	glucan	5 (A.ost.)	This study	n.s.
GH5_7	endo-β-1,4-mannanase	mannose	6	This study	4.9×10^{-7}
GH5_15	endo-β-1,6-glucanase	glucan	5 (S.com.)	This study	2.7×10^{-8}
GH5_49, GH5_9	endo-β-1,6-glucanase, exo-β-1,3-glucanase	glucan	6	Sakamoto et al 2017	1.3×10^{-3}
GH6	Exo-β-1,4-glucanase, cellobiohydrolase	glucan	5 (S.com.)	This study	n.s.
GH12_1	endo-β-1,4-glucanase	glucan	5 (A.ost.)	This study	2.6×10^{-3}

GH16	endo-β-1,3-1,4-glucanase	glucan	6	Sakamoto et al 2017	1.2×10^{-26}
GH16_2	endo-β-1,3-glucanase, endo-β-1,3-1,4-glucanase	glucan	5 (L.tig)	This study	1.2×10^{-26}
GH17	endo-β-1,3-glucanosyltransferase	glucan	6	This study	n.s.
GH18	chitinase	chitin	5 (L.tig)	This study	3.6×10^{-6}
GH18_5	chitinase	chitin	6	This study	3.6×10^{-6}
GH30_3	endo-β-1,6-glucosidase	glucan	6	Sakamoto et al 2017	2.7×10^{-14}
GH71	endo-β-1,3-glucanase	glucan	5 (P.chr.)	This study	1.6×10^{-7}
GH79_1	β-glucuronidase	unknown	4 (P.chr. S.com.)	This study	1.7×10^{-52}
GH92	α-1,3-mannosidase	mannose	5 (S.com.)	This study	2.1×10^{-18}
GH128	endo-β-1,3-glucanase	glucan	5 (P.chr.)	Sakamoto et al 2017, 2011	n.s.
GH152	β-1,3-glucanase, thaumatin	glucan	6	This study	2.0×10^{-18}
PL5	alginate lyase	?	6	This study	9.17×10^{-04}
PL14-like	alginate lyase-like	?	6	This study	8.5×10^{-19}
Expansins	cellulose/chitin loosening	chitin	6	Sipos et al 2017	1.5×10^{-94}
Kre9/Knh 1	Glucan remodeling	glucan	6	Szeto et al 2007	1.5×10^{-05}

Only families that are developmentally regulated in 5 or 6 species are shown (except GH79). Conservation of the developmental regulation is given as the number of species in which a given family is developmentally regulated followed by the name(s) of species in which ther ewere no developmentally regulated members. Gene family expansion in the Agaricomycetes was tested by a Fisher exact test, and considered significant at $P < 0.05$. For the Kre9/Knh1 family, P-value refers to the overrepresentation of the corresponding InterPro domain.